Engineering Solid Mechanics 11 (2023) 437-446

Contents lists available at GrowingScience

Engineering Solid Mechanics

homepage: www.GrowingScience.com/esm

# Influence of chemical composition of soda ash activated fly ash and copper slag geopolymer pastes on compressive strength

**Ibukun Olubusola Erunkulu[a*], Goitseone Malumbela[a] and Oluseyi Philip Oladijo[b]**

[a]*Department of Civil and Environmental Engineering, Botswana International University of Science and Technology, Botswana*
[b]*Department of Chemical, Materials and Metallurgical Engineering, Botswana International University of Science and Technology, Botswana*

**ARTICLEINFO**

*Article history*:
Received 10 January 2023
Accepted 21 April 2023
Available online
21 April 2023

*Keywords*:
*Geopolymer*
*Alkaline activation*
*Fly ash, Copper slag*
*Soda ash*
*Paste characterization*
*Compressive strength*

**ABSTRACT**

The effect of the chemical composition of geopolymer pastes on compressive strength was investigated in high-calcium fly ash and copper slag blends. In synthesizing the pastes, soda ash at activator to binder ratio of 0.4 was used. The characterization of material samples and the hardened fly ash-copper slag pastes was conducted through X-ray fluorescence (XRF), and X-ray diffraction (XRD) for the major oxide and phase composition. The hardened paste cubes which were cured at 80 °C were tested for compressive strength at ages 3, 7, and 28 days to obtain the mechanical performance property of each respective mix. The findings establish the impact of variation in the individual material and paste composition on the compressive strength of fly ash-copper slag geopolymer. The result shows that increase in the $SiO_2/Al_2O_3$ and $Na_2O/Al_2O_3$ ratios of paste products of samples corresponded to an increase in compressive strength. Whilst $Fe_2O_3$ wt.% increase in products from slag addition and positively influenced the compressive strength as fillers. However, CaO had no positive influence on the matrix of the activated product. The optimal blend mix design was 40 wt.% of copper slag which achieved a 28-day compressive strength of 24.66 MPa.



## 1. Introduction

In line with sustainable development goals, geopolymer, and alkaline-activated materials are green alternatives considered for cement replacement given the high $CO_2$ emission linked to its production. Cement production processes account for around 8 percent of global carbon emission (Olivier, Janssens-Maenhout, Muntean, & Peters, 2016) with an anticipated increase as the demand for cement in construction rises globally. Geopolymers and alkaline-activated materials (AAM) synthesized from the reaction of alkaline solution with aluminosilicates at regulated or ambient temperatures present one of the applicable solutions to the current concerns. Since aluminosilicate sources within industrial wastes, which pose environmental disposal challenges can be utilized, the potentials therein are immense. The synthesis of binders with cementitious properties under this class of material has been extensively investigated in several studies (Aliabdo, Abd Elmoaty, & Emam, 2019; Bernal, Nicolas, van Deventer, & Provis, 2015; de Oliveira et al., 2022; Dludlu, Oboirien, & Sadiku, 2017; Ishwarya, Singh, Deshwal, & Bhattacharyya, 2019; Komnitsas, Zaharaki, & Perdikatsis, 2007; Li, Ma, Zhang, & Zheng, 2013; Matalkah, Xu, Wu, & Soroushian, 2017; Nodehi & Taghvaee, 2022; Suwan & Fan, 2017; Yan et al., 2021) exhibiting equivalent or better mechanical properties, reduced shrinkage, and exceptional durability where the listed parameters were studied (Provis, Palomo, & Shi, 2015). These specified performance indicators, however, are dependent on a few variables, including precursor reactivity, alkaline activators, curing conditions, and mix procedures or techniques.

* Corresponding author.
E-mail addresses: ibukunerunkulu@gmail.com (I. O. Erunkulu)

ISSN 2291-8752 (Online) - ISSN 2291-8744 (Print)

doi: 10.5267/j.esm.2023.4.002

As part of the underlying factors influencing the final synthesized geopolymer product, the reactivity of precursors is affected by their chemical composition (Fernández-Jiménez & Palomo, 2003). Commonly used precursors such as fly ash (Nath, Maitra, Mukherjee, & Kumar, 2016), granulated blast furnace slag (GBFS) (Bernal, Provis, Mejía de Gutiérrez, & van Deventer, 2014) and metakaolin (Valentini, 2018) have different reactivity based on the reactive elements in their glassy phases (Ogundiran & Kumar, 2016). Precursors with higher silica and alumina contents typically have higher reactivity because they have a greater number of reactive sites that can take part in the creation of the geopolymeric network (J. L. Provis & Van Deventer, 2009). The reactivity of precursors can also be influenced by other elements like calcium, magnesium, and iron. These elements can combine to produce oxides that can also participate in geopolymerization, although their high concentrations can cause undesired phases to develop and weaken the final product. A study by (Cho, Jung, & Choi, 2019) has shown the ratio of network-forming Si, Al, and Fe to network-modifying Ca, Mg, Na, and K is one of the key factors of fly ash's reactivity and the products' compressive strength. The study also concludes that there was a significant correlation between the chemical parameters derived from chemical composition and compressive strength.

Consequent to these findings, blended geopolymeric binders produced through the hybridization of binary or ternary industrial aluminosilicate sources in alkaline activation are widely researched presently since C-S-H gel and geopolymeric gel can co-exist (Part, Ramli, & Cheah, 2017). The underlying concept is in the alteration of the Ca/Si and Si/Al ratios by utilizing calcium-rich precursors such as class C fly ash and GBFS in conjunction with other waste to achieve better setting time and significant early gain in strength. The role of calcium, silica, and alumina is highly relied on in this system. (Ukritnukun, Koshy, Rawal, Castel, & Sorrell, 2020) investigated the influence of slag content on the setting time and compressive strength of fly ash-blast furnace slag-based geopolymer. The proportioning ratio of fly ash to slag significantly affected compressive strength and no strength increase was recorded at slag content greater than 50%. (Nath & Kumar, 2013) examined the effect of the addition of two types of slags (GBFS and corex) on the geopolymerization reaction and the resulting structural rearrangement. New mineral phases and gels were formed which translated in compressive strength. Noting that both slag types used in the above studies are high calcium slag with similar composition, the understanding of this effect when other slag types like low calcium and iron-rich slag are used in conjunction with fly ash is required particularly with lower alkaline activators.

Activation of copper slag can be challenging because of some inert composition. Though in lesser quantity in comparison with other precursors such as blast furnace slag and fly ash, the slag type still contains $SiO_2$, $Al_2O_3$, and CaO in their glassy phase (Part et al., 2017). Considering that studies on copper slag activation are pale in comparison to the afore mentioned precursors, the minute essential oxides as well as the effect of high $Fe_2O_3$ content could be a possible explanation. Since in the synthesis mechanism, the role played by competing reactions and impurities such as iron species from source materials is still being studied (Ukritnukun et al., 2020). Often classified as impurity in precursors, the development in strength of activated product is viewed to be impaired by high iron composition in source material. (Nath & Kumar, 2013) however reported the presence of crystalline iron phases did not mitigate against the formation of geopolymers with excellent compressive strength in NaOH activation of volcanic ash, rather their effect was associated with the iron oxidation state. It will therefore be of interest to assess these effects with moderate alkaline activators such as sodium carbonate in the potential it presents for development where copper slag is the readily available aluminosilicate material.

The pH of alkaline activation systems being an important factor in reaction product development, the initial lower pH of sodium carbonate aqueous solution in the range of 11 may be inadequate in promoting early dissolution of the aluminosilicate glass. However, the efficiency of sodium carbonate activation can be maximized through an exchange reaction between carbonate ions and calcium ions facilitated by the introduction of calcium-rich compounds. The exchange reaction results in a steady rise in the pH of pore liquid from newly formed calcium carbonate and the equivalent release of hydroxyl (Yuan, 2017). For instance, a recent study by (Brykov & Voronkov, 2023) found the pH of the system to attain up to 14 when sodium carbonate is mixed with high-calcium fly ash in water medium in the activation of ground blast furnace slag. The rise in pH and the resulting compressive strength of the developed mortar were features of the exchange reaction and the resulting high alkaline medium. With these positive outcomes, the potential in the use of sodium carbonate activator in fly ash and copper blends can be explored if there are similarities in the observation.

Based on the limited study on the adoption of fly ash and copper slag blends in geopolymer synthesis and cases of activation with mild alkaline activator, the correlation of the chemical composition of the product is therefore essential. Understanding the relationship link in chemical composition and compressive strength can provide valuable insights into the optimization of these waste material components in the activation process. Therefore, this study aimed to determine the effect of the chemical composition of soda ash activated fly ash and copper slag geopolymer pastes on compressive strength. This is achieved through the characterization of pastes products by pH, X-ray diffraction (XRD), X-ray fluorescence (XRF) coupled with compressive strength tests.

## 2. Materials and methods

### *2.1. Source Material and Activator*

The source materials in the geopolymer synthesis are fly ash and copper slag. The samples were obtained from Morupule power plant and BCL copper and nickel mine in Botswana for fly ash (MBFA) and copper slag (CS) respectively. Prior to

use, the bulk fly ash sample was sieved both as a cleaning process and to obtain fine particles in the range shown in Figure 1(b). The copper slag sample was pulverised in a planetary ball mill and sieved for very fine particles less than 45 microns that can enhance reactivity. The activator in this study is soda ash (sodium carbonate). Soda ash dense grade produced by Botash with 99.5% $Na_2O$ and a pH of 11.03 in solution at room temperature. Being in granules, the soda ash was milled prior to use in activation. Table 1 highlights the chemical composition for all the materials used. Given the calcium content, the ash is a high calcium ash while the copper slag is low calcium slag which also contains high amounts of iron.

**Table 1**. Source material and activator composition

| Oxide (%) | MB fly ash | Copper slag | Soda ash |
|---|---|---|---|
| $SiO_2$ | 33.28 | 23.89 | - |
| $Al_2O_3$ | 26.16 | 5.26 | - |
| CaO | 20.54 | 2.72 | - |
| $Fe_2O_3$ | 6.82 | 59.10 | - |
| $SO_3$ | 8.52 | 2.12 | - |
| MnO | 0.21 | 0.05 | - |
| $Na_2O$ | 0.61 | 0.81 | 99.50 |
| MgO | 1.17 | 2.80 | - |
| $TiO_2$ | 1.95 | 0.29 | - |
| $K_2O$ | 0.32 | 0.74 | - |

### *2.2. Characterization of source material and hardened geopolymer paste*

Laser diffraction Malvern Mastersizer 3000 was used for particle size analysis for the fly ash and slag samples. The liquid dispersion method which is highly suitable for samples consisting of very fine particles in low micron range was used with water as the dispersant. The obtained distribution of particle sizes in both materials is shown in Figure 1. The milled copper slag is characterized by higher finer particles compared to the fly ash. Below 45 μm, the particle size was 89.81wt.% and 92.92 wt.% respectively for MBFA and milled copper slag. Multimodal distribution is observed in the fly ash implying the presence of multiple size groups within the sample. Whereas the copper slag sample shows a much better particle size distribution ranging between values as low as 0.2 μm and as high as 100 μm.

The sample chemical composition and phases was determined by X-ray fluorescence spectroscopy (S8 Tiger Bruker) and X-ray diffraction (Bruker D8 advance X-ray diffractometer). For the XRF analysis, each sample was run three times per observation during the test and further analysed with Spectra Plus software. X-ray diffraction was carried out on samples using Cu Kα radiation with wavelength (λ) of 1.54Å. The XRD traces were measured from 8° to 90° 2θ at a 0.02° 2θ step size while the generator runs at 40 kV and 40 mA. The degree of crystallinity for pasted samples was determined using the Match! software and the amorphous content were calculated using Eq. 1. The X-ray diffraction curve and phase composition of the fly ash and copper slag are shown in Fig. 2. Between the two precursors, the fly ash appears to be more crystalline overall in comparison with the copper slag. As seen from the diffraction pattern, the copper slag is amorphous without clearly distinctive diffraction peaks typical of crystalline materials. Though slightly amorphous at a range of 10 to 20° theta, crystalline peaks of mullite, quartz, lime and anhydrite were however observed in the fly ash sample. The presence of lime validates the XRF analysis in Table 1, which showed fly ash to contain a high percentage of CaO. To conclude chemical characterization, the pH of the source material and hardened pastes was measured with an Orion Star A111 pH meter from the milled fragments which were dissolved in water.

$$\text{Amorphous content (wt.\%)} = 100 - \text{degree of crystallinity} \tag{1}$$

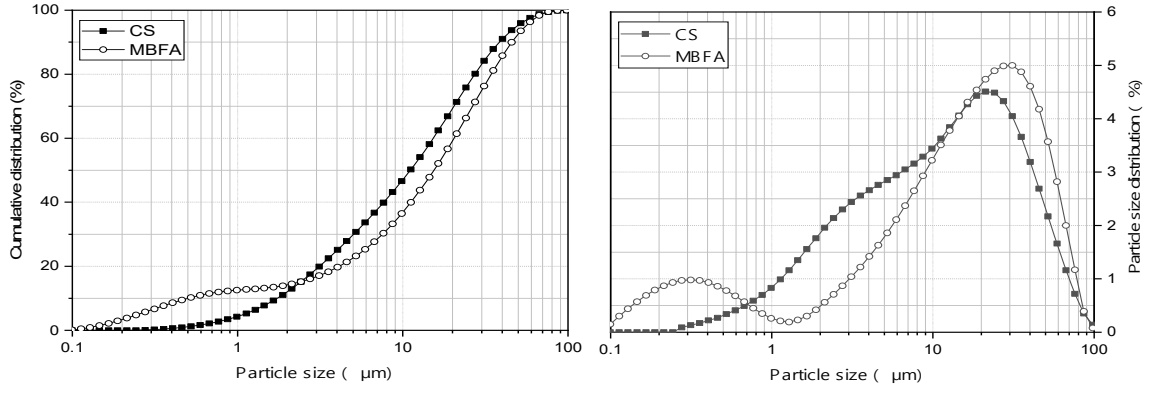


**Fig. 1.** (a) Cumulative distribution and (b) Particle size distribution of CS and MBFA

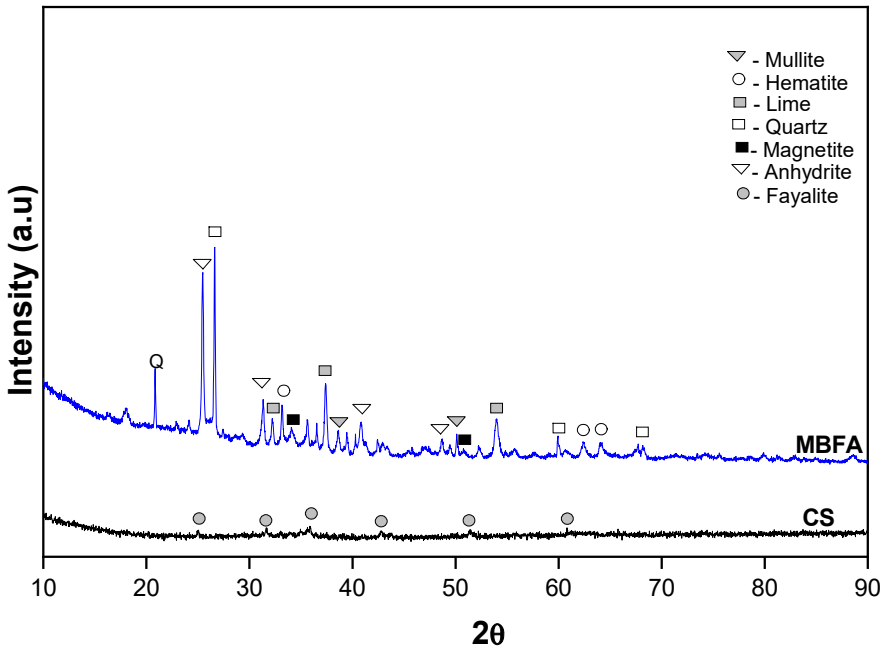


**Fig. 2.** Phase identification of fly ashes and copper slag by XRD

*2.3. Experimental design*

The experimental mix design undertaken in this study is shown in Table 2. Five mix designs were derived with variation in the fly ash to copper slag ratio. The parameters considered in the experiment include precursor mix ratio (FA/CS), curing temperature (80 °C), activator to binder ratio (0.40), liquid-to-solid ratio (L/S), and curing duration (3, 7, 28 days). The solid herein is the combination of the fly ash, copper slag and the soda ash mass. For workability, the L/S of the 100 % fly ash mix was slightly adjusted due to the stiffness of the mix with L/S of 0.3.

**Table 2.** Experimental mix design details

| Material | Mix type | | | | |
|---|---|---|---|---|---|
| | MBGP1 | MBGP2 | MBGP3 | MBGP4 | MBGP5 |
| Fly ash (% source material) | 100 | 80 | 70 | 60 | 50 |
| Copper slag (% source material) | 0 | 20 | 30 | 40 | 50 |
| Soda ash (% mass of Source material) | 40 | 40 | 40 | 40 | 40 |
| Water (liquid-to-solid ratio) | 0.438* | 0.3 | 0.3 | 0.3 | 0.3 |

*2.4 Paste Preparation*

The paste preparation process is as detailed in (Erunkulu, Malumbela, & Oladijo, 2022). Geopolymer pastes samples from the blends were synthesized from the mix design details given in Table 2. The initial stages for the one-part activation include blending the weighted fly ash and copper slag in a Hobart mixer for 3 mins at a slow speed of 140 rpm. Soda ash was then introduced in dry form into the material blend and further mixed at 200 rpm for 2 mins. Water was gradually added to the homogeneous mix while mixing for 3 mins at the same speed till all materials were well incorporated. Subsequently, the freshly mixed fly ash-copper slag geopolymer pastes were cast in 50 mm cube steel moulds. Based on a nomenclature generated from mix composition and fly ash source, the geopolymer samples were labelled. For example, MBGP4 is a sample made from 50% MBFA and 50% CS. After resting for an hour, the samples were transferred to a preheated electric oven maintained at 80 °C. and were demoulded after 24 hrs. The curing temperature was observed for the first 3 days for all geopolymer samples before being stored at room temperature till the required day of testing.

*2.5. Testing of compressive strength*

Servohydraulic testing machine with a load capacity of 600 kN was used in the compressive strength test setup. The load was applied at 0.9 kN/s until sample failure and values recorded. The test was carried out on the fly ash-copper slag geopolymer cube samples at ages 3, 7 and 28 days. As per ASTM C109, an average of three cubes samples per mix type were used for the observation. Fragmented pieces from the tests were then stored for other analysis and characterization.

## 3. Results and discussion

### *3.1 Sample Efflorescence*

Geopolymers contain high concentrations of soluble alkali metal, therefore efflorescence could be a major issue during exposure to moisture or humid air. Excess alkali presence is therefore a tendency for efflorescence formation (Z. Zhang, Provis, Reid, & Wang, 2014). The hardened paste samples in this study exhibited initial mild efflorescence formation as seen in Fig. 3, as well as the crystallization of salt on the mould during the first 24 hours of heat curing, because of soluble $Na^+$ ion in the evaporated water. However, efflorescence in these samples was lower than those associated with NaOH activation (Ishwarya et al., 2019). Similar efflorescence observation reported in (Erunkulu, Malumbela, & Oladijo, 2023) for blends of copper slag and low calcium fly ash activation. The degree of formation on geopolymer is also dependent on the alkali metal in the activators. For instance, sodium based activators are prone to yield more efflorescence (Lv, Qin, Lin, Tian, & Cui, 2020) due to the smaller size and higher charge density of $Na^+$ ions. Given the nature of the surface deposit, the initially high soda ash content used in this study, which was necessitated by the poor reactivity of source material contributed to the efflorescence. The excess $Na_2O$ in the fly ash-copper slag geopolymer matrix pore solution migrates through the pores and evaporates from the geopolymer surface leaving deposits.

The synthesized fly ash- copper slag geopolymer samples exhibited different efflorescence and was observed to decrease with copper slag addition. That is higher observations were made in samples with higher fly ash composition. Noting the migratory nature of the $Na^+$ ions in the pore solution, the higher L/S ratio used in the preparation of the 100 % fly ash mix may have contributed to the efflorescence in this sample. A result of rapid evaporation of free water and the formation of pores in the process. According to the study by (Zhang et al., 2014) on efflorescence in fly ash-based geopolymers, compositional change resulting from slag addition can mitigate efflorescence formation. This is from the formation of higher gel volume and compact microstructure with the addition of slag. In the absence of microscopy analysis, these features can also be related to sample strength in the with mixes in this study. Therefore, the observation on efflorescence characteristics for MBGP4 and MBGP5 which are mixes of high slag composition are valid.

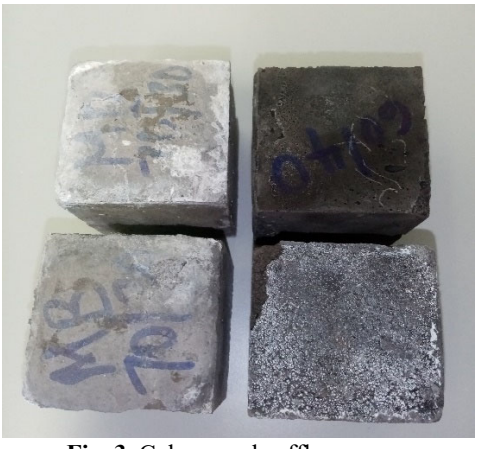

**Fig. 3.** Cube sample efflorescence

### *3.2. pH*

The pH values of pastes samples in a dilute solution are compared against their respective compressive strength in **Fig. 4.** The highlight of the study was the activation of precursors with a mildly alkaline activator (soda ash) below pH 11. The average pH value across the paste mixes is 10.3. Contrary to the findings by (Brykov & Voronkov, 2023) in their activation of HCFA-GGBFS with sodium carbonate, there was no increase in the pH of the product which had been attributed to possible ion exchange. For instance, mixes MBGP1 and MBGP2 which were high fly ash volume mixes exhibited lower pH amongst the pastes. Although the efficiency of the reaction had been hinged on the capability of the materials to release $Ca^{2+}$ readily as the reaction occurs. The same may not have been the case in these FA-CS mixtures. The product pH values for samples tested after 28 days were found to be proportional to the $Na_2O$ % content obtained in the chemical composition analysis of the paste samples, which are also proportional to the compressive strength. The result shows that as the $Na_2O$ % content increases, the pH value of the sample increases and vice versa. Since the pastes, the differences in the pH recorded within the paste's matrices could be due to the source material blend, as the $Na_2O$ in copper slag was higher than in fly ash. (Risdanareni, Puspitasari, & Januarti Jaya, 2017) established a correlation between material pH value and CaO content, the pH was reported to increase with CaO. The observations of this study in Table 3 are different and are rather directly linked with the $Na_2O$ composition.

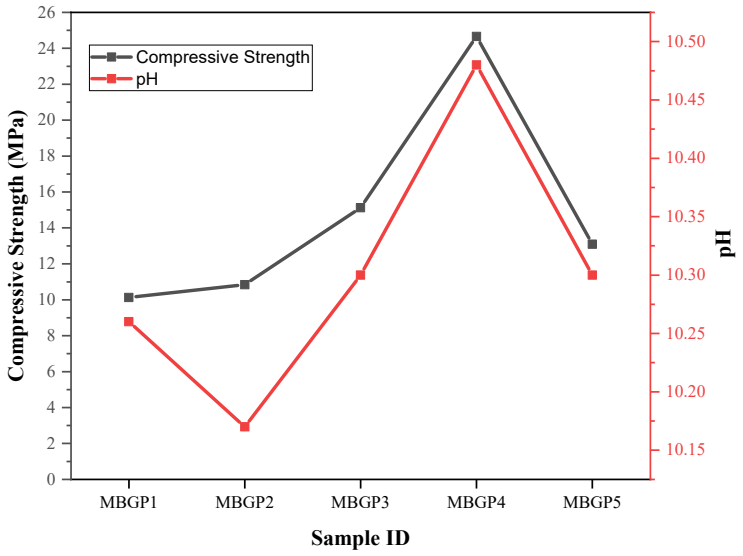


**Fig. 4.** Sample pH value and compressive strength relations

*3.3. XRD*

The results from the XRD analysis of the activated fly ash and copper pastes are presented in **Fig. 5.** From the diffraction patterns of the FACS pastes, there is a significant difference in the development of observed phases both in quality and quantity including transformations from the source material. The hydration products comprise the formation of new phases as nepheline and Na, Ca, Al, and Si hydrate of low crystallinity. Each paste exhibited a different degree of amorphousness and higher values of 97.26 %, 97.64 %, and 97.78 % were observed for MBGP3, MBGP4, and MBGP5 respectively. MBGP1 pastes made from sole fly ash activation retained most of the crystalline phases in MB fly ash and the highest degree of crystallinity within the mix. This could be indicative of less participation of Si and Al in some crystalline forms like quartz within the mix matrix. Although the intensity of quartz decreased significantly with copper slag addition, the presence of magnetite phases in the fly ash remained unchanged in activated pastes as reported in an earlier study by (Ishwarya et al., 2019). Also not participating in the reaction according to (T. Zhang et al., 2020) and current observation is the fayalite mineral phase present in the copper slag, which remained unchanged both in position and intensity. There is however the dissolution of mullite and anhydrite phases from the fly ash material as shown by their absence in all pastes. Diffraction patterns of MBGP3, 4, and 5 are very similar in comparison to the others and could explain the closer compressive strength values obtained from the three mixes which would be because of the similarity in structure. The slight change in the MBGP1 diffraction pattern suggests the presence of bulk unreacted fly ash particles as geopolymers are known to contain unreacted solid source materials (Duxson et al., 2005).

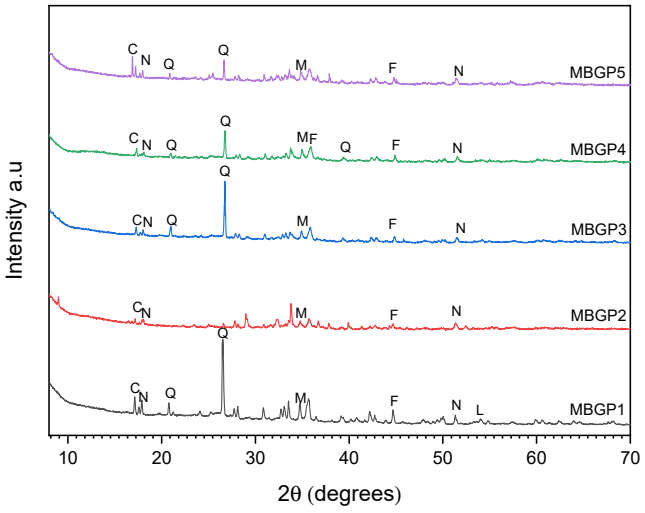


**Fig. 5.** XRD patterns of soda ash-activated fly ash-copper slag geopolymer

(C = C-Na-Al-S-H, Q = quartz, M = magnetite, N = Nepheline, L = lime, F = fayalite)

### *3.4. XRF*

XRF analysis was used to observe the changes in the oxide composition of activated pastes, the result is presented in Table 3. The percentage of major oxide is in the order $SiO_2$> $Na_2O$> $Fe_2O_3$ >$Al_2O_3$>CaO for most of the mixes except MBGP1 which had the lowest iron oxide content being a sole fly ash-activated product. Clearly, some increased constituents in pastes such as $Fe_2O_3$ and $Na_2O$ are due to the addition of copper slag and soda ash activation, which increased the values significantly. Though the silica contents of the different pastes were found to be proportional to the volume of fly ash.

As reported by (Singh, Ishwarya, Gupta, & Bhattacharyya, 2015), the properties of geopolymer pastes are affected most importantly by the following ratios: $SiO_2/Al_2O_3$, $R_2O/Al_2O_3$, and $SiO_2/R_2O$, where R is either of $Na^+$ or $K^+$, depending on the activator alkali metal. The Silica to alumina ($SiO_2/Al_2O_3$) ratio of paste samples in the range of 1.39-1.57, which increased with slag addition was correlated with compressive strength. Reaction products in the paste MBGP4 sample tagged with a better performance presented the highest ratio of 1.57 among the mixes and the lowest value of 1.39 obtained from MBGP1. With an increasing $SiO_2$/ $Al_2O_3$ ratio, the compressive strength of samples increased. The reduction in the percentage of silica and alumina content of the pastes shows their participation in the formation of new phases (Ishwarya et al., 2019). Another chemical composition ratio $Na_2O/Al_2O_3$ showed a positive response in activated pastes. The values increased with $Na_2O$ content and are found to be in the range of 0.94-1.51, higher than the range obtained by (Ishwarya et al., 2019) which were deemed adequate for strength development. For $SiO_2/Na_2O$ ratio, the compressive strength relationship inferred from the result is that an increase in $Na_2O$ content or decrease in $SiO_2$ correlated to an increase in strength. That is, the compressive strength increases with a decrease in the value of this ratio.

Despite the high calcium composition in sample mixes, the presence of weak C-S-H peaks and the absence of Ca $(OH)_2$ in the diffractograms of products suggests that the calcium from MBFA (class C fly ash) did not readily dissolve in soda ash activator as prevalent in GBFS activation. (Ukritnukun et al., 2020) implied that high calcium slag-based systems such as GBFS yielded higher levels of crystalline C-S-H and that the high calcium content in class C fly ash seemed to reduce the matrix strength. This agrees with the observation of this study wherein the MBGP1 sample with the highest CaO wt.% of 19.5 recorded the lowest compressive strength. Notably, the compressive strength of samples was seen to increase with the reduction in CaO content across the mixes. (Oh, Monteiro, Jun, Choi, & Clark, 2010; Sasui, Kim, Nam, Koyama, & Chansomsak, 2020) suggested that due to the difference in chemical forms of calcium in class C fly ash and GBFS, the calcium in the slag is readily available to form C-S-H gels while it is not in class C fly ash. Therefore, the CaO measured in the samples of this study is likely to be in the stated unavailable calcium forms.

The importance of iron is also illustrated by the values presented in Table 3. Though the iron crystalline phases in the figure were unreacted and remained unchanged in position, the Fe2O3 wt.% composition of samples from the table and compressive strength values of samples shows increasing strength with iron content. The change in strength trend at 50 % copper slag replacement in MBGP5 alludes to this, as the iron oxide content decreased from 21.9 % in MBGP4 to 19 % in MBGP5. These are consistent with the findings of (Nath & Kumar, 2013; Obonyo et al., 2014), which proposed that $Fe_2O_3$ acts as foreign nucleation during reaction including nanofillers within the pore structure of the matrix.

**Table 3.** Oxide composition of activated pastes

| Oxide (%) | MBGP1 | MBGP2 | MBGP3 | MBGP4 | MBGP5 |
|---|---|---|---|---|---|
| $SiO_2$ | 27.00 | 25.10 | 23.00 | 22.70 | 23.60 |
| $Al_2O_3$ | 19.40 | 16.60 | 15.30 | 14.50 | 15.70 |
| CaO | 19.50 | 15.10 | 12.40 | 11.80 | 13.70 |
| $Fe_2O_3$ | 6.43 | 15.20 | 20.80 | 21.90 | 19.00 |
| $SO_3$ | 6.06 | 5.22 | 4.20 | 3.90 | 4.60 |
| $Na_2O$ | 18.20 | 19.60 | 20.50 | 21.90 | 20.00 |
| MnO | 0.22 | 0.17 | 0.14 | 0.13 | 0.15 |
| MgO | 1.18 | 1.14 | 1.18 | 1.20 | 1.18 |
| $SiO_2$/ $Al_2O_3$ | 1.39 | 1.51 | 1.50 | 1.57 | 1.50 |
| $Na_2O$/ $Al_2O_3$ | 0.94 | 1.18 | 1.34 | 1.51 | 1.27 |
| $SiO_2$/ $Na_2O$ | 1.48 | 1.28 | 1.12 | 1.04 | 1.18 |

### *3.5. Compressive Strength*

The results of the compressive strength test obtained for the five mix types at 3, 7, and 28 days are shown in Figure 6 and previously in Figure 4. The figure shows the strength development with age in the fly ash-copper slag geopolymer is congruent with those from earlier studies (Bernal et al., 2015; Erunkulu et al., 2022) on alkaline-activated systems. Compressive strength in this study increases with copper slag addition and reaches an optimum in the mix MBGP4. At high fly ash volume, however, due to unreacted bulk material, depolymerization occurs slowly in the material (T. Zhang et al., 2020). Consequently, the lowest compressive strength is observed in mixes MBGP1 and 2, and a slower early strength development rate of 34.73 % and 49.23 % between age 3 and 7 days of samples. Pore formation within the MBGP1 matrix due to more free water from the adjusted water-to-binder ratio compared to other mixes may also have contributed to the results. Despite the low compressive strength in this mix, the values are however higher than those reported by (Park, Seo, & Lee, 2018) for the similar fly ash activation with $Na_2CO_3$.

Under the same curing condition, MBGP4 attained the optimum strength of 24.66 MPa at day 28. as well as an observed early strength gain of nearly 300 % from 3 to 7 days of sample age, which may be a result of better binder gel formation within the matrix (Park et al., 2018). Although the sample failed to gain significant strength after 7 days, an increase of just about 1 % was attained at 28 days compared to other samples which gained an average of 20 % from the 7 days compressive strength.

The change in strength appears the most dramatic between 40 % and 50 % slag addition. The decrease in compressive strength between MBGP4 and MBGP5 indicates that other factors begin to influence the strength of the sample. Overall, in all the paste samples, $Na_2CO_3$ (soda ash) activation yields a low early age strength due to the slow dissolution of silicate and alumina species from the initial low pH of the system (Bernal et al., 2015; Bernal, Provis, Myers, San Nicolas, & van Deventer, 2014).

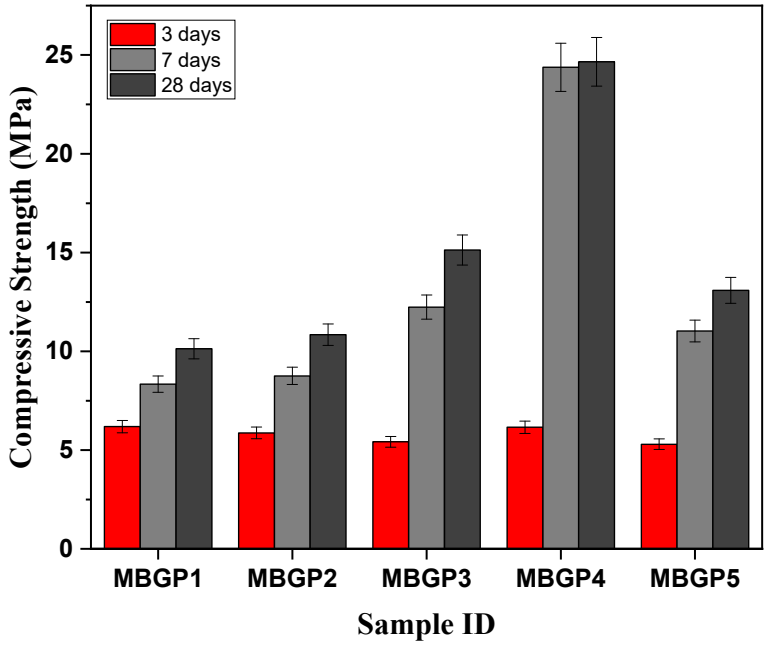


**Fig. 6.** Compressive strength of fly ash-copper slag geopolymer pastes

## 4. Conclusion

The current study examines the influence of chemical composition on the compressive strength of soda ash-activated fly ash-copper slag pastes. Soda ash activation of fly ash and copper slag in varying blends produced material with different structures. The results from the characterization of paste products give insight into the chemical composition effect in mild alkaline activated systems and the roles played by precursor blends in composition variation. The following are the summarised findings.

1. Hardened fly ash-copper slag geopolymers exhibited mild efflorescence formation which became less prominent after 28 days of samples. Geopolymers with high copper slag volume barely exhibited efflorescence. This is because the inclusion of copper slag to the matrix creates a change in composition which mitigated surface discoloration.
2. The pH of Fly ash-copper slag geopolymers products due to soda ash activation was low (an average of 10.3). Individual sample pH was found to be a function of the $Na_2O$ composition present in the product. The values increased with increasing $Na_2O$ wt.% and were higher in mixes with high copper slag volume. This was linked to the compressive strength of the samples.
3. XRD patterns showed the sample with sole fly ash activation had the highest degree of crystallinity which was retained from the raw fly ash material used. This implied the presence of unreacted material with soda ash activation, whereas the higher amorphousness in samples with copper slag indicated a better reaction including the transformation of phases. Iron phases from copper slag were retained in Fly ash-copper slag geopolymers with slag addition.
4. $SiO_2$/ $Al_2O_3$ and $Na_2O/Al_2O_3$ ratios from the chemical composition of fly ash-copper slag geopolymers products were both indicative of better activation results. The ratios increased with compressive strength; highest in the mix with 40 % slag composition and lowest in the mix with no slag addition. CaO content in paste products did not influence compressive strength positively and was inversely proportional, high content of 19.5 % still resulted in low strength. Therefore, the Ca content of the material in this study is postulated to be in an unavailable form for C-S-H gel formation.

5. Iron oxide composition in fly ash-copper slag geopolymers increased with slag addition but positively influenced the compressive strength of samples in that unreacted forms may have functioned as fillers in the microstructure of the paste samples.
6. Early strength development in Fly ash-copper slag geopolymers soda ash activation was low. A maximum strength of 24.66 MPa was achieved at 28 days in a mix comprising 60% and 40% of fly ash and copper slag respectively when heat cured at 80 °C. Important chemical features in this optimum blend mix include highest $SiO_2$/ $Al_2O_3$, highest $Na_2O/Al_2O_3$, highest $Fe_2O_3$, and the lowest $SiO_2/Na_2O$ in product composition.

## Acknowledgment

This research was supported by the Office of Research, Development, and Innovation (ORDI) of the Botswana International University of Science and Technology under grant S00177. The industry support through the provision of soda ash from Botash Pty. Ltd., fly ash by BPC, and copper slag by BCL for this research is also acknowledged by the authors.

## References

Aliabdo, A. A., Abd Elmoaty, A. E. M., & Emam, M. A. (2019). Factors affecting the mechanical properties of alkali activated ground granulated blast furnace slag concrete. *Construction and Building Materials*, *197*, 339–355. https://doi.org/10.1016/j.conbuildmat.2018.11.086

Bernal, S. A., Nicolas, R. S., van Deventer, J. S. J., & Provis, J. L. (2015). Alkali-activated slag cements produced with a blended sodium carbonate/sodium silicate activator. *Advances in Cement Research*, *28*(4), 262–273. https://doi.org/10.1680/jadcr.15.00013

Bernal, S. A., Provis, J. L., Mejía de Gutiérrez, R., & van Deventer, J. S. J. (2014). Accelerated carbonation testing of alkali-activated slag/metakaolin blended concretes: effect of exposure conditions. *Materials and Structures/Materiaux et Constructions*, *48*(3), 653–669. https://doi.org/10.1617/s11527-014-0289-4

Bernal, S. A., Provis, J. L., Myers, R. J., San Nicolas, R., & van Deventer, J. S. J. (2014). Role of carbonates in the chemical evolution of sodium carbonate-activated slag binders. *Materials and Structures/Materiaux et Constructions*, *48*(3), 517–529. https://doi.org/10.1617/s11527-014-0412-6

Brykov, A., & Voronkov, M. (2023). Dry Mix Slag — High-Calcium Fly Ash Binder . Part One : Hydration and Mechanical Properties. *Materials Sciences and Applications*, *14*, 240–254. https://doi.org/10.4236/msa.2023.143014

Cho, Y. K., Jung, S. H., & Choi, Y. C. (2019). Effects of chemical composition of fly ash on compressive strength of fly ash cement mortar. *Construction and Building Materials*, *204*, 255–264. https://doi.org/10.1016/j.conbuildmat.2019.01.208

de Oliveira, L. B., de Azevedo, A. R. G., Marvila, M. T., Pereira, E. C., Fediuk, R., & Vieira, C. M. F. (2022). Durability of geopolymers with industrial waste. *Case Studies in Construction Materials*, *16*(November 2021), e00839. https://doi.org/10.1016/j.cscm.2021.e00839

Dludlu, M. K., Oboirien, B., & Sadiku, R. (2017). Micostructural and Mechanical Properties of Geopolymers Synthesized from Three Coal Fly Ashes from South Africa. *Energy and Fuels*, *31*(2), 1712–1722. https://doi.org/10.1021/acs.energyfuels.6b02454

Duxson, P., Provis, J. L., Lukey, G. C., Mallicoat, S. W., Kriven, W. M., & Van Deventer, J. S. J. (2005). Understanding the relationship between geopolymer composition, microstructure and mechanical properties. *Colloids and Surfaces A: Physicochemical and Engineering Aspects*, *269*(1–3), 47–58. https://doi.org/10.1016/j.colsurfa.2005.06.060

Erunkulu, I. O., Malumbela, G., & Oladijo, O. P. (2022). Influence of Blend Ratio on Compressive Strength of Soda Ash Activated Fly Ash and Copper Slag Pastes. *7th International Conference on Civil, Structural and Transportation Engineering (ICCSTE'22)*, *3*(207), 1–12. https://doi.org/10.11159/iccste22.207

Erunkulu, I. O., Malumbela, G., & Oladijo, O. P. (2023). Feasibility of geopolymer synthesis using soda ash in copper slag blended fly ash-based geopolymer. *Materials Today: Proceedings*. https://doi.org/10.1016/j.matpr.2023.02.208

Fernández-Jiménez, A., & Palomo, A. (2003). Characterisation of fly ashes. Potential reactivity as alkaline cements. *Fuel*, *82*(18), 2259–2265. https://doi.org/10.1016/S0016-2361(03)00194-7

Ishwarya, G., Singh, B., Deshwal, S., & Bhattacharyya, S. K. (2019). Effect of sodium carbonate/sodium silicate activator on the rheology, geopolymerization and strength of fly ash/slag geopolymer pastes. *Cement and Concrete Composites*, *97*, 226–238. https://doi.org/10.1016/j.cemconcomp.2018.12.007

Komnitsas, K., Zaharaki, D., & Perdikatsis, V. (2007). Geopolymerisation of low calcium ferronickel slags. *Journal of Materials Science*, *42*(9), 3073–3082. https://doi.org/10.1007/s10853-006-0529-2

Li, X., Ma, X., Zhang, S., & Zheng, E. (2013). Mechanical properties and microstructure of class C fly ash-based geopolymer paste and mortar. *Materials*, *6*(4), 1485–1495. https://doi.org/10.3390/ma6041485

Lv, X. Sen, Qin, Y., Lin, Z. X., Tian, Z. K., & Cui, X. M. (2020). Inhibition of Efflorescence in Na-Based Geopolymer Inorganic Coating. *ACS Omega*, *5*(24), 14822–14830. https://doi.org/10.1021/acsomega.0c01919

Matalkah, F., Xu, L., Wu, W., & Soroushian, P. (2017). Mechanochemical synthesis of one-part alkali aluminosilicate hydraulic cement. *Materials and Structures/Materiaux et Constructions*, *50*(1), 97 (1-10). https://doi.org/10.1617/s11527-016-0968-4

Nath, S. K., & Kumar, S. (2013). Influence of iron making slags on strength and microstructure of fly ash geopolymer.

*Construction and Building Materials*, *38*, 924–930. https://doi.org/10.1016/j.conbuildmat.2012.09.070

Nath, S. K., Maitra, S., Mukherjee, S., & Kumar, S. (2016). Microstructural and morphological evolution of fly ash based geopolymers. *Construction and Building Materials*, *111*, 758–765. https://doi.org/10.1016/j.conbuildmat.2016.02.106

Nodehi, M., & Taghvaee, V. M. (2022). Alkali-Activated Materials and Geopolymer: a Review of Common Precursors and Activators Addressing Circular Economy. *Circular Economy and Sustainability*, *2*(1), 165–196. https://doi.org/10.1007/s43615-021-00029-w

Obonyo, E. A., Kamseu, E., Lemougna, P. N., Tchamba, A. B., Melo, U. C., & Leonelli, C. (2014). A sustainable approach for the geopolymerization of natural iron-rich aluminosilicate materials. *Sustainability (Switzerland)*, *6*(9), 5535–5553. https://doi.org/10.3390/su6095535

Ogundiran, M. B., & Kumar, S. (2016). Synthesis of fly ash-calcined clay geopolymers: Reactivity, mechanical strength, structural and microstructural characteristics. *Construction and Building Materials*, *125*, 450–457. https://doi.org/10.1016/j.conbuildmat.2016.08.076

Oh, J. E., Monteiro, P. J. M., Jun, S. S., Choi, S., & Clark, S. M. (2010). The evolution of strength and crystalline phases for alkali-activated ground blast furnace slag and fly ash-based geopolymers. *Cement and Concrete Research*, *40*(2), 189–196. https://doi.org/10.1016/j.cemconres.2009.10.010

Olivier, J. G. J., Janssens-Maenhout, G., Muntean, M., & Peters, J. (2016). Trends in Global CO2 Emissions: 2016 Report;© PBL Netherlands Environmental Assessment Agency: The Hague. In *PBL Netherlands Environmental Assessment Agency*. https://doi.org/https://www.pbl.nl/en/trends-in-global-co2-emissions

Park, S. M., Seo, J. H., & Lee, H. K. (2018). Binder chemistry of sodium carbonate-activated CFBC fly ash. *Materials and Structures/Materiaux et Constructions*, *51*(3), 59(1-10). https://doi.org/10.1617/s11527-018-1183-2

Part, W. K., Ramli, M., & Cheah, C. B. (2017). An Overview on the Influence of Various Factors on the Properties of Geopolymer Concrete Derived From Industrial Byproducts. In *Handbook of Low Carbon Concrete*. https://doi.org/10.1016/B978-0-12-804524-4.00011-7

Provis, J. L., & Van Deventer, J. S. J. (2009). Introduction to geopolymers. In *Geopolymers: Structures, Processing, Properties and Industrial Applications*. https://doi.org/10.1533/9781845696382.1

Provis, John L., Palomo, A., & Shi, C. (2015). Advances in understanding alkali-activated materials. *Cement and Concrete Research*, Vol. 78, pp. 110–125. https://doi.org/10.1016/j.cemconres.2015.04.013

Risdanareni, P., Puspitasari, P., & Januarti Jaya, E. (2017). Chemical and Physical Characterization of Fly Ash as Geopolymer Material. *MATEC Web of Conferences*, *97*. https://doi.org/10.1051/matecconf/20179701031

Sasui, S., Kim, G., Nam, J., Koyama, T., & Chansomsak, S. (2020). Strength and microstructure of class-C fly ash and GGBS blend geopolymer activated in NaOH & NaOH + Na2SiO3. *Materials*, *13*(1). https://doi.org/10.3390/ma13010059

Singh, B., Ishwarya, G., Gupta, M., & Bhattacharyya, S. K. (2015). Geopolymer concrete: A review of some recent developments. *Construction and Building Materials*, *85*, 78–90. https://doi.org/10.1016/j.conbuildmat.2015.03.036

Suwan, T., & Fan, M. (2017). Effect of manufacturing process on the mechanisms and mechanical properties of fly ash-based geopolymer in ambient curing temperature. *Materials and Manufacturing Processes*, *32*(5), 461–467. https://doi.org/10.1080/10426914.2016.1198013

Ukritnukun, S., Koshy, P., Rawal, A., Castel, A., & Sorrell, C. C. (2020). Predictive model of setting times and compressive strengths for low-alkali, ambient-cured, fly ash/slag-based geopolymers. *Minerals*, *10*(10), 1–21. https://doi.org/10.3390/min10100920

Valentini, L. (2018). Modeling Dissolution-Precipitation Kinetics of Alkali-Activated Metakaolin [Research-article]. *ACS Omega*, *3*(12), 18100–18108. https://doi.org/10.1021/acsomega.8b02380

Yan, Z., Sun, Z., Yang, J., Yang, H., Ji, Y., & Hu, K. (2021). Mechanical performance and reaction mechanism of copper slag activated with sodium silicate or sodium hydroxide. *Construction and Building Materials*, *266*, 1–14. https://doi.org/10.1016/j.conbuildmat.2020.120900

Yuan, B. (2017). *Sodium carbonate activated slag : reaction analysis , microstructural modification & engineering application*. Eindhoven University of Technology, the Netherlands.

Zhang, T., Jin, H., Guo, L., Li, W., Han, J., Pan, A., & Zhang, D. (2020). Mechanism of Alkali-Activated Copper-Nickel Slag Material. *Advances in Civil Engineering*, *2020*. https://doi.org/10.1155/2020/7615848

Zhang, Z., Provis, J. L., Reid, A., & Wang, H. (2014). Fly ash-based geopolymers: The relationship between composition, pore structure and efflorescence. *Cement and Concrete Research*, *64*, 30–41. https://doi.org/10.1016/j.cemconres.2014.06.004